Lysophosphatidic acid signaling during embryo development in sheep: Involvement in prostaglandin synthesis

Ewa E. Liszewska, Pierrette P. Reinaud, Emmanuelle Billon-Denis, Olivier O. Dubois, Philippe Robin, Gilles Charpigny

Lysophosphatidic Acid Signaling during Embryo Development in Sheep: Involvement in Prostaglandin Synthesis

Ewa Liszewska, Pierrette Reinaud, Emmanuelle Billon-Denis, Olivier Dubois, Philippe Robin, and Gilles Charpigny

INRA (E.L., P.Re., O.D., G.C.), UMR 1198 Biologie du Développement et Reproduction, F-78350 Jouy en Josas, France; and Institut de Biochimie et Biophysique Moleculaire et Cellulaire (E.B.-D., P.Ro.), Centre National de la Recherche Scientifique, Unité Mixte de Recherche 8619, Equipe Signalisation et Régulations Cellulaires, Université Paris-Sud, F-91400 Orsay, France

We investigated the lysophosphatidic acid (LPA) pathway during early pregnancy in sheep. LPA was detected in the uteri of early-stage pregnant ewes. Using quantitative RT-PCR, the expression of autotaxin, the LPA-generating enzyme, was found in the endometrium and conceptus. In the latter autotaxin, transcript levels were low on d 12–14 and increased on d 15–16, in parallel with the level of LPA. Autotaxin was localized in the luminal epithelium and superficial glands of the endometrium and in trophectoderm cells of the conceptus. The expression of G protein-coupled receptors for LPA was also examined in the ovine conceptus. LPA receptor LPAR1 and LPAR3 transcripts were expressed during early pregnancy and displayed a peak on d 14, whereas the highest level of protein for both receptors was observed at d 17. LPAR1 was localized in cellular membranes and nuclear compartments of the trophectoderm cells, whereas LPAR3 was revealed only in membranes. LPA activated phosphorylation of the MAPK ERK1/2 in ovine trophectoderm-derived cells. Moreover, the bioactive lipid increased the proliferation of trophectoderm cells in culture, as shown by thymidine and bromodeoxyuridine incorporation. Furthermore, LPA induced changes to the organization of β-actin and α-tubulin, suggesting a role for it in rearrangement of trophectoderm cells cytoskeleton. Because a link had previously been established between prostaglandin and LPA pathways, we analyzed the effect of LPA on prostaglandin synthesis. LPA induced an increase in the release of prostaglandin F2α and prostaglandin E2, with no significant modifications to cytosolic phospholipase A2α and prostaglandin synthase-2 expression. Taken together, our results suggest a new role for LPA-mediated signaling in the ovine conceptus at the time of implantation. **(*Endocrinology* 150: 422–434, 2009)**

Lysophosphatidic acid (LPA) is a naturally occurring, small phospholipid. LPA exerts a broad range of biological actions, such as cell proliferation, differentiation, migration, invasion, adhesion, survival, and morphogenesis (1), and it plays several roles in female reproductive physiology (2). In rodents, LPA has been reported to be involved in oocyte maturation (3). In mice, LPA has been implicated in tubal transport of the ovum (4) and the preimplantation development of embryos (5). More recently the LPA signaling pathway was demonstrated as exerting an influence on mouse embryo implantation (6). LPA is produced extracellularly in the serum and plasma, mainly from lysophosphatidylcholine by a secreted lysophospholipase-D, which has been identified as autotaxin (7). Autotaxin, also known as ectonucleotide pyrophosphatase/phosphodiesterase 2 (ENPP2), is an exoenzyme that was initially identified as a tumor cell autocrine motility factor (8). Autotaxin has phosphodiesterase and phospholipase activities and has been demonstrated to be a secreted enzyme (9) that catalyzes the production of LPA in extracellular body fluids (10).

LPA acts on target cells through six specific G protein-coupled receptors (LPARs), LPAR1-6 (11). LPAR1-3 are structurally related and were originally described as members of the

ISSN Print 0013-7227 ISSN Online 1945-7170
Printed in U.S.A.

doi: 10.1210/en.2008-0749 Received May 19, 2008. Accepted August 26, 2008.
First Published Online September 4, 2008

Abbreviations: BrdU, Bromodeoxyuridine; cPLA, cytosolic phospholipase A; DAPI, 4′,6-diamidino-2-phenylindole; EDG, endothelial differentiation gene family; ENPP2, ectonucleotide pyrophosphatase/phosphodiesterase 2; GAPDH, glyceraldehyde-3-phosphate dehydrogenase; LPA, lysophosphatidic acid; LPAR, LPA receptor; PB, phosphate buffer; PG, prostaglandin; PTGS2, prostaglandin synthase-2.

so-called endothelial differentiation gene family (EDG). Nearly all mammalian cells, tissues, and organs coexpress several LPAR subtypes. LPAR1 is the most widely expressed receptor, with high levels in the brain, colon, heart, placenta, small intestine, and prostate. LPAR2 and LPAR3 exhibit a more restricted distribution pattern and are found in the testes, kidney, heart, lung, and brain. The other two identified LPARs (LPAR4 and LPAR5) and the recently discovered LPAR6 are distinct from LPA-EDG receptors (12, 13). High levels of LPAR4 mRNA have been found in human ovary, whereas in mice, LPAR5 is expressed at low levels in most tissues. The great variety of cellular and biological actions of LPA can be explained by the broad tissue distribution of LPARs and their coupling to several types of G proteins (Gq, Gi, Gs, G12/13) (14). LPA binding to cell membrane receptors influences several signaling routes, including the inhibition/activation of adenyl cyclase, the activation of phosphatidyloinositol-3-kinase, the induction of the mitogenic Ras-MAPK cascade, the stimulation of phospholipase C, and activation of the Rho kinase family.

The activation of ERK(1/2) MAPK is reported to be a widely observed effect after LPAR1-3 activation (15). Genetic null mouse studies have revealed the importance of the biological functions of LPARs, particularly in embryo development (16). The targeted deletion of LPAR1 in mice resulted in about 50% of lethality, with surviving animals showing reduced size and other abnormalities (17), whereas no obvious phenotype abnormalities were found in mice lacking LPAR2 (18). The deletion of LPAR3 results in delayed embryo implantation; reduced litter size, probably due to defects in implantation; altered embryo spacing; and embryo crowding (6). In mice lacking LPAR3, expression of the rate-limiting enzyme in prostaglandin production, prostaglandin synthase-2 (PTGS2), is markedly reduced with lower levels of prostaglandin E_2 (PGE_2) and PGI_2. The implantation phenotype of LPAR3-deficient mice has been reported to be similar to that observed in mice deficient in cytosolic phospholipase A 2α (cPLA2α) (19) and PTGS2 (20). Because the principal implantation defects were restored by an exogenous administration of prostaglandin, it has been considered that cPLA-2α, PTGS2, and LPAR3-mediated signaling have a crucial role in embryo implantation through prostaglandin signaling. In ruminants, as in other species, implantation is the result of a complex series of interactions between the trophectoderm and the maternal endometrium. Unlike human and mouse blastocysts, the hatched ruminant blastocyst remains detached from the uterus and undergoes dramatic morphological changes before implantation. In sheep, rapid expansion of the trophectoderm transforms the spherical blastocyst at d 10 into a tubular form on d 11–12, and a filamentous conceptus between d 13 and 16. This elongation process leads to a 15-cm-long ovine conceptus and initiates the implantation phases, which, successively, involve apposition and transient attachment and then firm adhesion by d 16–17 (21, 22).

To date, LPA-mediated signaling has been deemed to play a crucial role in mouse embryo implantation through the uterine LPAR3 receptor. In domestic mammals, the expression of the LPAR3 receptor in uterus has been reported only in pig (23, 24). No data are available describing the LPA pathway in embryos during the periimplantation period. During this study, we examined the key actors in the LPA signaling pathway at the time of the maternal recognition of pregnancy in the sheep. We measured LPA levels in the uterus and established the expression of autotaxin and LPAR1-3 receptors in the ovine uterus and conceptus.

Our results have identified an unique expression pattern of LPA receptors in the trophectoderm of the ovine conceptus. Because we previously evidenced developmentally regulated expression of PTGS2 in the sheep embryo (25), our purpose was to test the current hypothesis, which affirms that LPA signaling affects PTGS2 expression and prostaglandin synthesis. Using an ovine trophectoderm cell line, we showed that LPA increased the release of PGF2α, and we then evaluated the effect of LPA on cPLA2α and PTGS2 gene expression.

Materials and Methods

Animals and sample collection

All procedures relative to the care and use of animals were approved by the French Ministry of Agriculture and completed with French regulations (86/609/EEC updated April 19, 1988) concerning animal experimentation. Ewes of the Préalpes-du-Sud breed were synchronized as described previously (26), fertilized or not. The animals were slaughtered on d 12–15 of the estrous cycle and d 12–18 of pregnancy. Five to seven pregnant ewes at d 12–18 and four to five nonpregnant ewes at d 12–15 were used to investigate gene expression and protein studies in the uterine endometrium during early pregnancy and the estrous cycle, respectively. The uterus was removed and conceptuses were collected from pregnant ewes by flushing each uterine horn with 20 ml PBS at 38 C. The developmental stage and morphology of conceptuses were identified by binocular observation. Trophectoderms were obtained by dissecting the embryonic disc from the whole conceptus. A total of 65 conceptuses, obtained from three series of pregnant ewes, were collected from d 12 to d 18. When the conceptus size was large enough, the trophectoderms were divided into halves. An average of eight conceptuses per developmental stage were subjected to transcript analysis, and four to five per developmental stage were subjected to protein analysis using Western blotting. Endometrial tissues were dissected from the myometrium. Endometria and trophectoderms were frozen immediately in liquid nitrogen and stored at −80 C until RNA and protein extraction. Uterine flushes were clarified by centrifugation and stored at −20 C for lipid extraction. For immunohistochemistry, cross-sections of uterine horns and conceptus pieces were fixed in fresh 4% paraformaldehyde in PBS (pH 7.5). After washes in cold 0.1 M phosphate buffer (pH 7.5), the tissues were successively immersed in 15% (wt/vol) and 18% (wt/vol) sucrose in phosphate buffer, embedded in Shandon Cryomatrix (Thermo-Scientific, Courtaboeuf, France), frozen in liquid nitrogen vapor, and stored at −80 C.

Culture of trophectoderm cells

Trophectoderm cells were derived from d 16 conceptuses. The trophectoderm was dispersed mechanically by pipetting up and down through 1.2-mm-internal diameter needle. Small clumps of cells were plated on a rat collagen gel substratum and cultured in DMEM/F12 medium with 100 IU/ml penicillin, 100 μg/ml streptomycin, 250 IU/ml nystatin, 2.5 μg insulin, 1.25 μg/ml transferrin, and 1.25 ng/ml sodium selenite and supplemented with 10% (vol/vol) lipid-free fetal calf serum in a humidified atmosphere of 5% CO_2 at 38 C. The time of cell division and morphology remain stable during passages. The cells required 18–20 h to duplicate and were able to reach confluence after 7–8 d of culture. The presence of cytokeratin 7 proved the epithelial nature of the cells,

TABLE 1. Sequence of primers used for RT-PCR and quantitative real-time RT-PCR

Gene	Oligonucleotide primer sequences (5′ → 3′)		Product size (bp)	Annealing temperature (C)
	Forward	Reverse		
Semiquantitative RT-PCR				
Autotaxin	ACGATGGCTTACACGACACA	GTCTTGCGGAAGAAGTCCAG	298	62
LPAR1	CTCATTGACACCACCGTGAC	GTTGAAAATGGCCCAGAAGA	264	62
LPAR2	GGTCATCATGCTGATTGTGG	TCAGCGTTGTTTCACGGTAG	275	62
LPAR3	CCTGACCAAAAAGAGGGTGA	GCTGATGGACCCACTCGTAT	271	60
LPAR4	TTCCTGGCCATTGTCTATCC	GGAGGGTTTTTAGCACCACA	286	60
PTGS2	AGGTGTATGTATGAGTGTAGG	GTGCTGGGCAAAGAATGCAA	484	57
cPLA2α	GAGAAAGGGCCAGAGGAGAT	ATCGGGTTTGACATGGAGAC	279	60
GAPDH	TGTCCGTTGTGGATCTGACC	AGCCGAATTCATTGTCGTACC	151	60
Quantitative real-time RT-PCR				
Autotaxin	CGACAACGACGAGAGCTGC	TGAGATGCTCGATGTCCCG	101	60
LPAR1	ACGGTCATTCCGTATGCAGC	GGATAGCCCCCATGACGAT	101	60
LPAR2	TCTTCCTGCTCATGGTGGC	GCGTTGTTTCACGGTAGCG	111	60
LPAR3	TCCAACCTCATGGCCTTCTT	GACCCACTCGTATGCGGAGA	101	60
LPAR4	ATGCAACCACCACCTGCTTT	AGGAATGATAAAACCAACAACTTCAA	101	60
PTGS2	TCCGCCAACTTATAATGTGCAC	GGCAGTCATCAGGCACAGGA	101	60
cPLA2α	CTTCGGGATGTTAATAGGAGAAACA	GAGGCAAAGGACACTGTCCAG	101	60
GAPDH	TGTCCGTTGTGGATCTGACC	AGCCGAATTCATTGTCGTACC	151	60

whereas the absence of vimentin excluded the contamination of trophectoderm cells with cells of mesoderm origin. The trophectoderm nature of cells was confirmed by interferon-τ expression. The functional stability of the cells was verified throughout 35 passages by maintaining the expression of genes for prostaglandin and LPA pathways.

Radioenzymatic quantification of lysophosphatidic acid

Radioenzymatic quantification of LPA was performed as described previously (27). Lipid extraction from 10 ml of uterine flushes was performed with 1 vol butanol-1. After shaking and centrifugation (15 min at 2500 × *g*), the upper phase of butanol-1 was collected and evaporated under vacuum at 50 C. Dry samples were solubilized in 200 μl chloroform and stored at −20 C until LPA quantification by radioenzymatic assay. Chloroform was evaporated and dry lipid extracts were resuspended in 200 μl of 20 mM Tris (pH 7.5) in the presence of 20 μM sodium orthovanadate and 1 mg/ml Tween 20 and containing 8.6 10^{-10} mol of [^{14}C]oleoyl-CoA (58 mCi/mmol; PerkinElmer Life Sciences, Courtaboeuf, France) and 10 μl of 1 μg/μl of recombinant 1-acyl-*sn*-glycerol-3-phosphate acyltransferase enzyme prepared as previously described (28). The samples were incubated for 2 h at 20 C and vortexed every 15 min. The reaction was stopped by adding 400 μl of chloroform-methanol-12M hydrochloric acid (40:40:0.26) and centrifuged for 5 min at 3000 × *g*. The lower chloroform phase was collected and evaporated under vacuum. Dry samples were resuspended in 20 μl chloroform-methanol (1:1) and spotted on a silica gel thin-layer chromatography glass plate (Merck, Frontenay sous Bois, France). Lipids were separated by migration in a solvent mixture composed of chloroform-methanol-ammonium hydroxide-water [65:25:0.9:3 (vol/vol/vol/vol)]. The plates were exposed to imaging screens (Fujifilm Life Science, FSVT, Courbevoie, France), and the image was captured using a Fuji FLA-3000 to localize ^{14}C-labeled lipids. Known amounts of LPA standards were used on thin-layer chromatography as a reference to quantify the amount of LPA in samples.

Quantitative RT-PCR analysis of autotaxin and LPARs

Total RNA was extracted using the phenol-based method described previously (29). The concentration and purity of RNA samples were determined by spectrophotometry at 260 and 280 nm. To estimate RNA integrity, aliquots were electrophoretically separated in 1% agarose gel and visualized by staining with ethidium bromide. First-strand cDNA was synthesized from 1 μg of total RNA using Moloney murine leukemia virus reverse transcriptase and oligo-deoxythymidine primer (Invitrogen, Cergy Pontoise, France) in a total volume of 20 μl. Real-time PCR was carried out using the real time Applied 7000 PCR system (Applera France SA, Courtaboeuf, France) with 5% of the retro-transcribed product and 300 nM of gene-specific oligonucleotide primers in a total volume of 25 μl of mastermix SYBR Green reagent (Applera France). Primers (Table 1) were designed using Primer Express software (Applera France). Real-time PCR conditions were 2 min at 50 C and 10 min at 95 C, followed by 45 cycles of 15 sec at 95 C and 1 min at 60 C. To confirm that the quantitative results were reliable, the homogeneity of PCR products was verified by dissociation curve analysis. Four to seven independent trophectoderm and endometrium samples were analyzed for each developmental stage. Standard curves were produced in parallel with several dilutions of the purified PCR product used as a polymerase template. Real-time PCR data were normalized for differences using glyceraldehyde-3-phosphate dehydrogenase levels. Real-time PCR data were analyzed using 7000 System SDS software (Applera France).

Western blot analysis

Trophectoderm tissues and cells were homogenized in cold 50 mM HEPES (pH 7.4) lysis buffer containing 150 mM NaCl, 5 mM EDTA, 16 mM 3-[(3-cholamidopropyl)-dimethylammoniol]1-propane-sulfonate, 1 mM benzamidine-HCl, 1 mM phenylmethylsulfonyl fluoride, 10 μg/ml soybean trypsin inhibitor, 10 μg/ml leupeptin, 10 μg/ml aprotinin (10 μg/ml), 200 μM Na_3VO_4, and 100 mM NaF (Sigma-Aldrich, St. Quentin Fallavier, France). Samples standardized for protein with the Bio-Rad protein assay (Bio-Rad, Marnes-la-Coquette, France) were separated by 10% SDS-PAGE and electrotransferred onto a Hybond-P, polyvinylidene difluoride membrane (GE Healthcare, Orsay, France). Dedicated membranes with different quantities of extracts were generated with 25 μg of total protein for the immunodetection of LPAR1, LPAR3, and autotaxin and with 10 μg for ERK1/2 and phospho-ERK1/2. Blots probed with anti-phosphoERK1/2 antibody were stripped in 50 mM Tris/HCl, 2% sodium dodecyl sulfate, and 100 mM β-mercaptoethanol and reprobed with anti-ERK1/2 antibody. Different antibodies [anti-LPAR1(rabbit polyclonal EDG2 antibody used at a 1:500 dilution), Abcam, Paris, France], [anti-LPAR3 (rabbit polyclonal EDG7 antibody used at a 1:200 dilution), Abcam], [anti-autotaxin (rabbit polyclonal ENPP2 antibody used at a 1:1000 dilution), CosmoBio, Tokyo, Japan], [anti-phospho-ERK1/2 (mouse monoclonal phospho-ERK1/2 antibody used at a 1:1000 dilution), Cell Signaling Technology, Ozyme, St. Quentin en Yvelines, France], [anti-ERK1/2 (rabbit polyclonal ERK1/2 antibody used at a 1:5000 dilution), Santa Cruz, Tebu-Bio, Le Perray en

Yvelines, France], [antiglyceraldehyde-3-phosphate dehydrogenase (GAPDH; mouse monoclonal GAPDH antibody used at a 1:100), MAB 374; Chemicon, Interchim, Montluçon, France] were diluted in 20 mM Tris-HCl, 500 mM NaCl, 5% (wt/vol) low-fat milk, and 0.1% (wt/vol) Tween 20. Peroxidase-conjugated donkey antirabbit and antimouse IgG (Jackson ImmunoResearch, Interchim, Montluçon, France) were diluted to 1:100,000 and 1:40,000, respectively. Immunoreactive signals were revealed by the ECL Plus Western blotting detection kit (GE Healthcare), visualized using a Fuji film LAS-1000 camera system, and analyzed by Advanced Image Data Analysis software (FujiFilm Life Science, FSVT). The molecular weights of the proteins identified were calculated using the Prosieve color protein marker (BMA Product, Tebu-Bio, Le Perray en Yvelines, France). For immunoneutralization control experiments, LPAR1 and LPAR3 antibodies were presaturated with the peptide antigens that had been used to generate antibodies [LPAR1 synthetic peptide: DRSASSLNH TILAGVHSN; LPAR3 synthetic peptide: MNECHYDKRMDF (Cayman Chemical, SpiBio, Montigny le Bretonneux France)].

Immunohistochemistry

Immunohistochemistry was performed on 10-μm frozen tissue sections with the Vectastain Elite ABC peroxidase System (Vector, Abcys, Paris, France) as previously described (30). Slides were delipidated for 5 min with chloroform and were then rehydrated with 0.1 M phosphate buffer (PB) containing 0.2% (wt/vol) BSA. The sections were treated with an unmasking procedure in 10 mM citrate (pH 6) at 85 C for 10 min and then 30 min in 0.1% (vol/vol) hydrogen peroxide in H_2O to quench endogenous peroxidase activity. The same antibodies as for Western blots were used at dilutions of 1:200 (LPAR1), 1:400 (LPAR3), and 1:500 (autotaxin) in PBS containing 2% BSA (wt/vol) and 1% donkey serum. The sections were incubated overnight at 4 C with primary antibodies and then for 1 h with the biotinylated second antibody at 1:1000 (donkey antirabbit IgG antibody; Jackson ImmunoResearch). The avidin-biotin peroxidase complex was applied for 1 h and the staining reaction performed for 5 min in the presence of 3, 3′diaminobendizine hydrochloride (Sigma-Aldrich). As a negative control, primary antibodies were omitted. Slides were mounted with AquaPerm mounting medium (Thermo Electron France, Cergy Pontoise, France) and Entellan-new mounting medium (Merck VWR, Strasbourg, France). Photomicroscopy was captured using an Olympus DP50 microscope, a digital camera system and software (Olympus SA, Rungis, France).

Immunohistofluorescence

Frozen tissue sections (10 μm) from conceptus and uterine tissue, mounted on Superfrost Plus microscope slides (Menzel-Gläser, CML, Nemours, France), were delipidated for 5 min with chloroform and then rehydrated with 0.1 M PB containing 0.2% BSA and saponin 0.05%. The sections were incubated overnight at 4 C with LPAR1, LPAR3, and autotaxin antibodies diluted at 1:50, 1:100, and 1:125, respectively, in 0.1 M PB with 0.2% BSA, 0.05% saponin, and 0.01% donkey serum. Immunoreactive protein was detected using a fluorescein-conjugated donkey antirabbit IgG at a dilution of 1:200 (Jackson ImmunoResearch). Nuclei were stained for 5 min with 0.5 μg/ml 4′,6-diamidino-2-phenylindole (DAPI) in 0.1 M PB. The sections were rinsed in 0.1 M PB and 0.3% Tween 20 and mounted using a Vectashield mounting medium (Vector, Abcys). Trophectoderm cells from the *in vitro* culture were treated as described above but without the delipidation step. Cells were incubated with LPAR1 and LPAR3 antibodies at 1:100 and 1:125, respectively. Photomicroscopy was captured as described above. Immunoneutralization experiments were also performed to confirm the specificity of the LPAR1 and LPAR3 antibodies. The antibodies were presaturated as for Western blot experiments.

Activation of ERK1/2 by LPA in trophectoderm cells

Preconfluent cell cultures were starved of serum during 24 h in fresh medium supplemented with 0.1% fatty acid-free BSA (Sigma-Aldrich). The dose (0–50 μM) and time (0–30 min) effects of LPA treatment were analyzed. When tested, the antagonist of LPAR1-LPAR3, VPC32183 (Avanti, Coger, Paris, France) was added for a 30-min pretreatment period at a concentration of 10 μM. The cells were then treated for 30 min with 20 μM LPA (1-oleoyl-2-hydroxy-sn-glycero-3 phosphate sodium salt; Avanti, Coger). At the end of experiment, the cells were washed with ice-cold PBS, collected, centrifuged for 10 min at 10,000 rpm, and stored at −80 C before analysis. Three independent experiments with four dishes per condition were performed.

Cell proliferation assays

Thymidine-based cell proliferation assay

Trophectoderm cells were seeded in 12-well tissue-culture dishes and cultured as described above. Preconfluent cell cultures were starved of serum by means of culture for 24 h in fresh medium supplemented with 0.1% fatty acid-free BSA. The cells were then incubated for a further 24 h with different concentrations of LPA and finally exposed for 2 h to 0.5 μCi/ml tritiated-thymidine [thymidine-(methyl-^{3}H), 78.5 Ci/mmol; PerkinElmer Life Sciences]. The cells were washed with ice-cold PBS, precipitated with trichloroacetic acid, and dissolved in 0.1 M NaOH. The radioactivity of incorporated [^{3}H]thymidine was determined by liquid scintillation counting. Two independent experiments were performed with three dishes per LPA concentration tested.

Bromodeoxyuridine (BrdU)-based cell proliferation assay

Trophectoderm cells were grown to semiconfluence on glass coverslips coated with collagen. Cells were starved of serum for 24 h as described above and then incubated for 24 h with 20 μM LPA. BrdU (10 μM; *in situ* cell proliferation kit; Roche Diagnostics, Meylan, France) was added to the medium for the final hour of culture. Cells were fixed in cold ethanol for 5 min and treated with 2 N HCl. BrdU-labeled cells revealed by sequential incubation with anti-BrdU antibody at a dilution of 1:20 (Abcys) for 1 h, and antirat-IgG Texas-Red conjugated antibody (Jackson ImmunoResearch) for 1 h. Cell nuclei were stained with 0.5 μg/ml DAPI (Sigma-Aldrich). The coverslips were mounted on slides and photomicroscopy was captured as described above. Two independent experiments were performed with three dishes per condition. Ten fields of each dish were analyzed using Image Tool software [Image Tool version 2.0; University of Texas Health Science Center at San Antonio (http://ddsdx.uthscsa.edu/)].

Effect of LPA on cell morphology

Trophectoderm cells were grown to confluence on glass cover slips coated with collagen. After that, cells were starved for 24 h as described above. The cells were then treated or not with 20 μM LPA for 1 h and fixed 10 min with 4% paraformaldehyde in PBS. β-Actin was visualized using an 0.5 U/ml rhodamine-phalloidin probe according to the manufacturer's protocol (Molecular Probes, Invitrogen, Cergy Pontoise, France). α-Tubulin was detected by overnight incubation at 4 C with anti-α-tubulin mouse monoclonal antibody (Sigma-Aldrich) diluted 1:200 in 0.1 M PB containing 0.2% BSA, 0.05% saponine, and 0.01% donkey serum. The fluorescent signal of the protein was visualized with a fluorescein-conjugated donkey antimouse IgG at a dilution of 1:200 (Jackson ImmunoResearch). Photomicroscopy was captured as described above. Two independent experiments were performed with four dishes per condition.

Effect of LPA on arachidonic acid metabolism in trophectoderm cells

The effect of LPA on cyclooxygenase-derivatives of arachidonic acid was analyzed on cells starved of serum for 24 h before the experiment. Cells cultured in 60-mm dishes were incubated in 5 ml DMEM/F12 medium with 0.1% BSA and treated for 6 h with 0.5 μCi/ml [5,6,8,9,11,12,14,15(*N*)-3H] arachidonic acid (specific activity 180–240 Ci/mmol; PerkinElmer Life Sciences) and incubated with different concentrations of LPA. At the end of the incubation period, the cultured medium was collected, centrifuged, and acidified with 100 μl/ml 0.5 M citric acid. The culture medium was extracted by solvents and

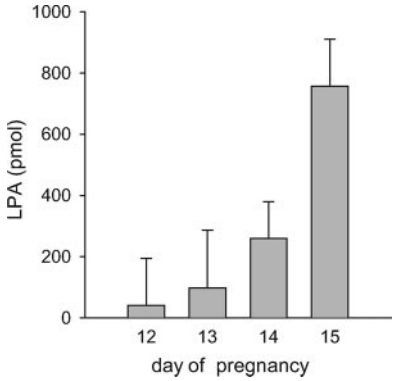

FIG. 1. LPA content in uterine flushings from pregnant ewes measured by radioenzymatic assay as described in *Materials and Methods* (n = 5 ewes/day of pregnancy). Low levels of LPA were found at d 12 of pregnancy, which then increased ($P = 0.038$) at d 15.

analyzed using the HPLC procedure described previously (31). Four samples per condition were analyzed. Based on dose-response experiments, 20 μM LPA was the dose selected for testing the effect of LPA on the expression of gene involved in prostaglandin synthesis. cPLA2α and PTGS2 mRNA was analyzed by quantitative RT-PCR as described above using primers indicated in Table 1. Four independent experiments were performed in triplicate.

Statistical analysis

Quantitative results were analyzed using one-way ANOVA with the SYSTAT software (GMBH, Erkrath, Germany). Data are presented as least squares mean ± SE.

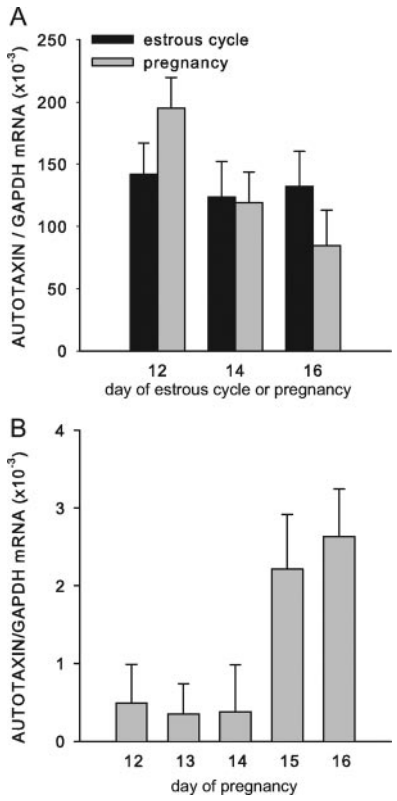

FIG. 2. Autotaxin transcript expression in the ovine endometrium during the estrous cycle and early pregnancy (A) and trophectoderm during conceptus development (B). A, Real-time quantitative RT-PCR analysis of the endometrium from d 12 to 16 of the estrous cycle and early pregnancy measured in duplicate. Autotaxin mRNA transcript levels were normalized to GAPDH (n = 5 ewes per status per day). Strong expression of the transcript was detected from d 12 to 16 without any significant differences between the pregnant and nonpregnant states ($P = 0.164$). B, Real-time quantitative RT-PCR analysis of three to five independent trophectoderm samples for each developmental stage measured in duplicate. Autotaxin mRNA transcript levels were normalized to GAPDH. Autotaxin was present from d 12 to 16 and the levels increased at d 15 and 16 ($P = 0.049$).

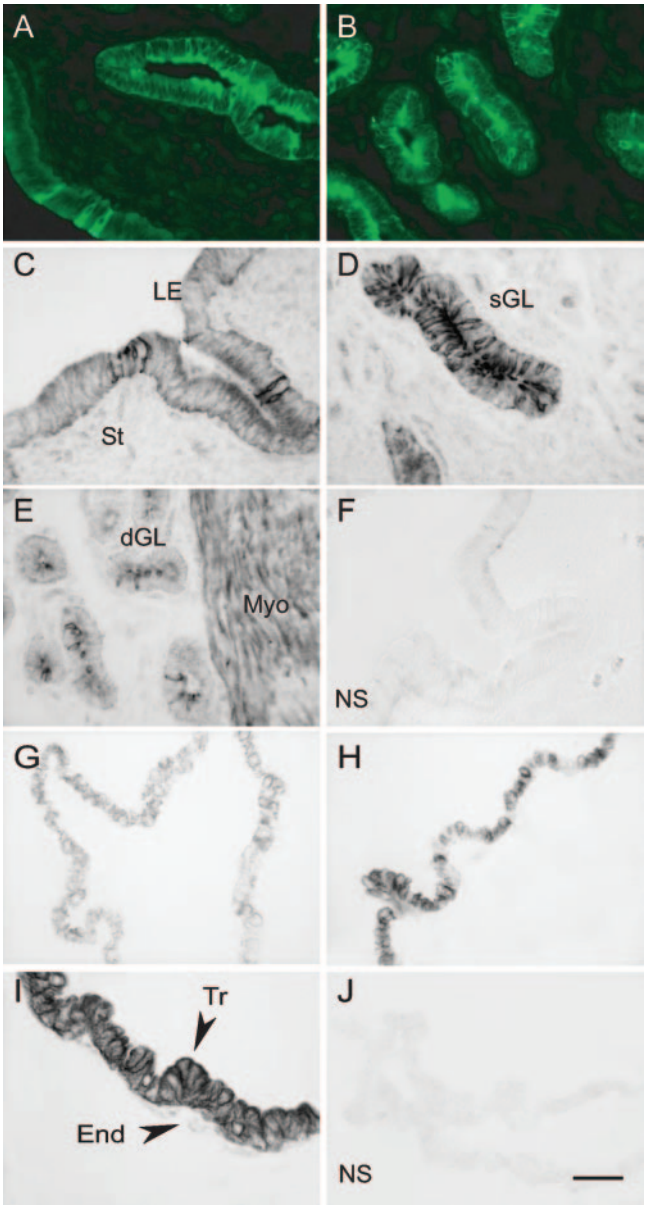

FIG. 3. Immunohistochemical localization of autotaxin in the uterus (A–E) and conceptus on d 12 (G), d 14 (H), and d 16 (I) of development. Representative transversal sections of uteri from d 14 of the estrous cycle (n = 5 tissue samples) and sections of conceptuses (n = 5 tissue samples per stage of development) were incubated with antiautotaxin polyclonal antibody and revealed by antirabbit-fluorescein isothiocyanate (A and B) or using a peroxidase Elite-ABC Vectastain kit and diaminobenzidine substrate (C–E and G–I). F and J, Negative controls: primary antibody was omitted in immunohistochemistry detection. LE, luminal epithelium; dGL, deep glands; sGL, superficial glands; St, stroma; Myo, myometrium; Tr, trophectoderm; End, endoderm. *Scale bar*, 50 μm. In endometrium, autotaxin was found in superficial glands, luminal epithelium, and deep glands. In conceptuses, autotaxin was detected in trophectoderm cells and levels increased between d 12 and 16.

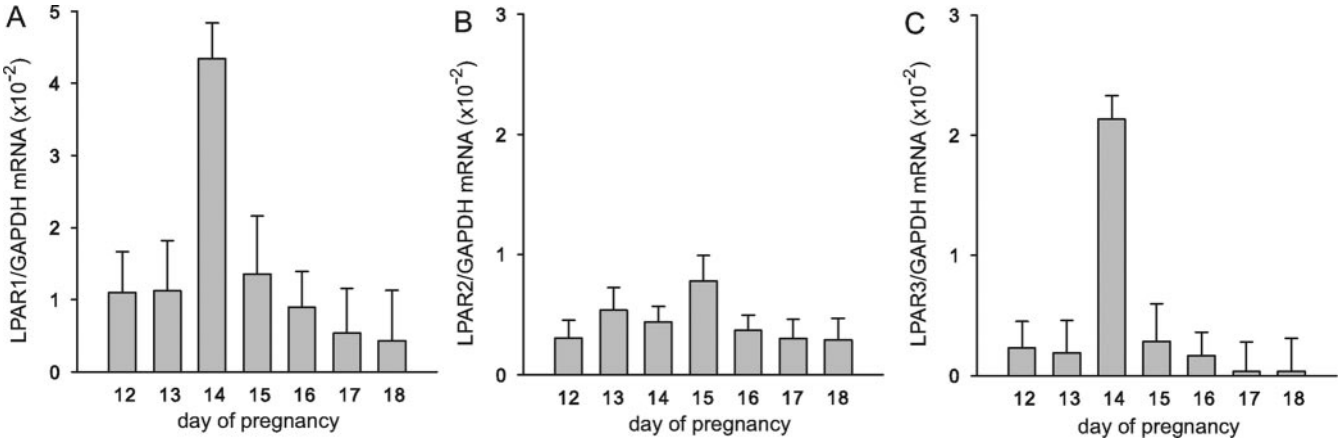

FIG. 4. LPAR1 (A), LPAR2 (B), and LPAR3 (C) transcript expression in ovine conceptus. Real-time quantitative RT-PCR analysis of three series of three to five conceptuses for each developmental stage measured in duplicate. The levels of each transcript were normalized to GAPDH expression. LPAR1, LPAR2, and LPAR3 were present in ovine conceptuses between d 12 and 18. LPAR1 and LPAR3 showed high increase in expression levels at d 14 ($P = 0.009$ and $P < 0.001$, respectively), whereas LPAR2 remained stable ($P > 0.05$).

Results

Presence of LPA in the ovine uterus

Local accumulations of LPA were detected in uteri of pregnant ewes. As illustrated in Fig. 1, low levels of LPA were found at d 12 of pregnancy, which then increased ($P = 0.038$) at d 15, reaching an average quantity of 700–800 pmol in the total flushing. Until d 14, similar levels were found in flushings from nonpregnant ewes (data not shown).

Expression of autotaxin in the ovine endometrium and trophectoderm

Using real-time RT-PCR analysis, we detected the expression of autotaxin in the endometrium and trophectoderm. In the endometrium (Fig. 2A), strong expression of the transcript was detected from d 12 to 16 without any significant differences between the pregnant and nonpregnant states ($P = 0.164$). In the trophectoderm (Fig. 2B), autotaxin was present from d 12 to 16 and the levels increased at d 15 and 16 ($P = 0.049$). The autotaxin transcript was much more strongly expressed in the endometrium (5000–8000 copies per 50 ng of RNA) than in the trophectoderm (100–1500 copies per 50 ng of RNA). The cellular localization of autotaxin protein was analyzed by immunohistochemistry. Figure 3, A–F, illustrates the uterine distribution of autotaxin on d 14 of the estrous cycle. Autotaxin was found in superficial glands. A weaker signal was also detected in the luminal epithelium, the deep glands, and the myometrium. In glands, autotaxin was mainly found at the apical pole of cells, close to the glandular lumen. These observations were better illustrated by immunofluorescence detection (Fig. 3, A and B) than by the immunoperoxidase technique. This localization of autotaxin is consistent with the secretory nature of the enzyme. In conceptuses (Fig. 3, G–J), autotaxin was weakly expressed in trophectoderm cells on d 12, but the levels then rose on d 14 and 16. Autotaxin was not detected in the extraembryonic endoderm (Fig. 3I).

LPARs in ovine conceptus

We examined the expression of four LPARs (LPAR1-4) in conceptuses from d 12 to 18 of development. Using semiquantitative and real-time RT-PCR, only the three related receptor subtypes, LPAR1, LPAR2, and LPAR3, were clearly evidenced in trophectoderm extracts. LPAR1 and LPAR3 were present at all developmental stages (Fig. 4, A and C) and displayed the same, precisely regulated, pattern of expression. Expression remained weak until d 13 (6000 and 800 copies per 50 ng of total RNA for LPAR1 and LPAR3, respectively), peaked at d 14 (70,000–80,000 copies for LPAR1 and 30,000–40,000 copies LPAR3 per 50 ng of RNA), and then declined (15,000 for LPAR1 and 1,000 for LPAR3; $P = 0.009$ and $P < 0.001$, respectively). The LPAR2 transcript was also expressed from d 12 to 18. Its level remained stable during the period analyzed (Fig. 4B). LPAR4 was not detected in significant amounts in trophectoderm extracts (<10 copies per 50 ng RNA). Western blot analysis of conceptus homogenates revealed a single band at the expected theoretical size of 40 kDa for both LPAR1 and LPAR3 (Fig. 5A, a and c). The preabsorption of LPAR1 and LPAR3 antibodies with the peptide antigen completely abolished the Western blot signals obtained with conceptus protein extracts (Fig. 5A, b and d), demonstrating the specificity of the antibodies used to detect LPAR1 and LPAR3. Figure 5, B and C, shows representative Western blots for LPAR1 and LPAR3 obtained from four to five individual conceptuses for each developmental stage between d 14 and 18. At d 14, the levels of both receptors were very low, rising between d 15 and 16 to reach a maximum at d 17 and then declining at d 18 ($P = 0.031$ and $P = 0.042$, respectively). Using immunofluorescence (Fig. 6, A and B), LPAR1 and LPAR3 receptors were localized in the trophectoderm of ovine conceptuses. Immunoreactivity for LPAR1 was detected in the cellular membranes and perinuclear/nuclear compartments of trophectoderm cells. By contrast, the LPAR3 receptor was observed only in the membrane of trophectoderm cells. Preabsorption of the antibodies with the peptide antigens resulted in the extinction of immunostaining (Fig. 6, C and D).

LPAR1 and LPAR3 receptors in a conceptus-derived trophectoderm cell line

We established an ovine trophectoderm cell line to assess the functionality of LPA on LPARs. Real-time PCR measurements

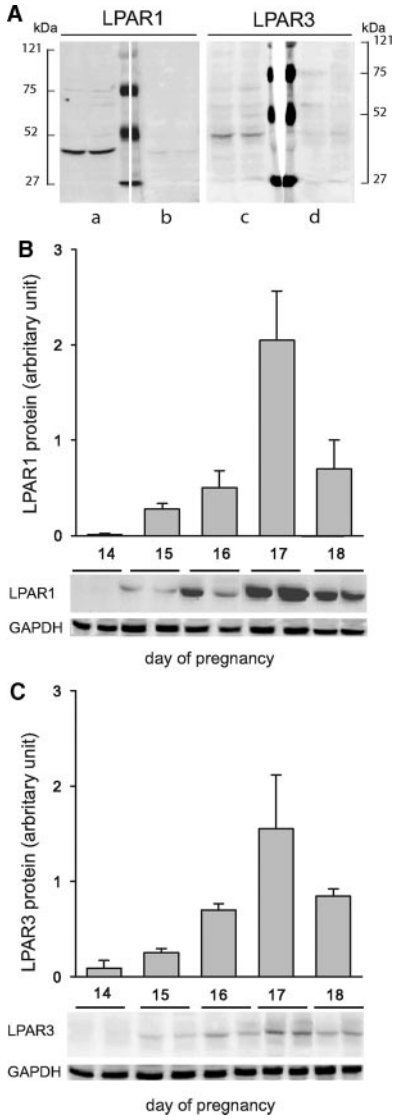

FIG. 5. Western blot analyses of LPAR1 and LPAR3 proteins in ovine conceptuses. A, Using polyclonal antibodies, two immunoreactive bands at about 40–43 kDa and corresponding to the predicted band sizes were detected for LPAR1 (a) and LPAR3 (c), respectively, in ovine conceptuses at d 16. Immunoneutralization experiments were performed to evaluate specific binding in Western blotting. LPAR1 and LPAR3 antibodies were neutralized by incubation with an excess of the peptides used to raise the polyclonal antibodies. The resulting Western blot shows an absence of bands corresponding to LPAR1 (b) and LPAR3 (d) proteins. B and C, Graphs show integrated signals of LPAR1 and LPAR3 proteins in four to five conceptuses per developmental stage. Representative Western blots of LPAR1 (B) and LPAR3 (C) in two conceptuses per day of pregnancy. After detection of LPARs, membranes were stripped and reprobed with antibody anti-GAPDH to confirm equal loading of samples on the gel. LPAR1 and LPAR3 proteins were observed in conceptuses between d 14 and 18 with maximum level at d 17 ($P = 0.031$ and $P = 0.042$, respectively).

showed that trophectoderm cells stably expressed transcripts of LPAR1 and LPAR3 receptors over the period of subculture. The receptors were expressed at levels comparable with these found in conceptuses on d 16 (data not shown). Immunohistochemical analysis confirmed the presence of LPAR1 and LPAR3 receptors in trophectoderm cells in culture (Fig. 6, E and F). As observed in the conceptus, LPAR1 was localized in both the cytoplasm and nuclear/perinuclear areas, whereas the LPAR3 receptor was found only in the cytoplasmic compartment.

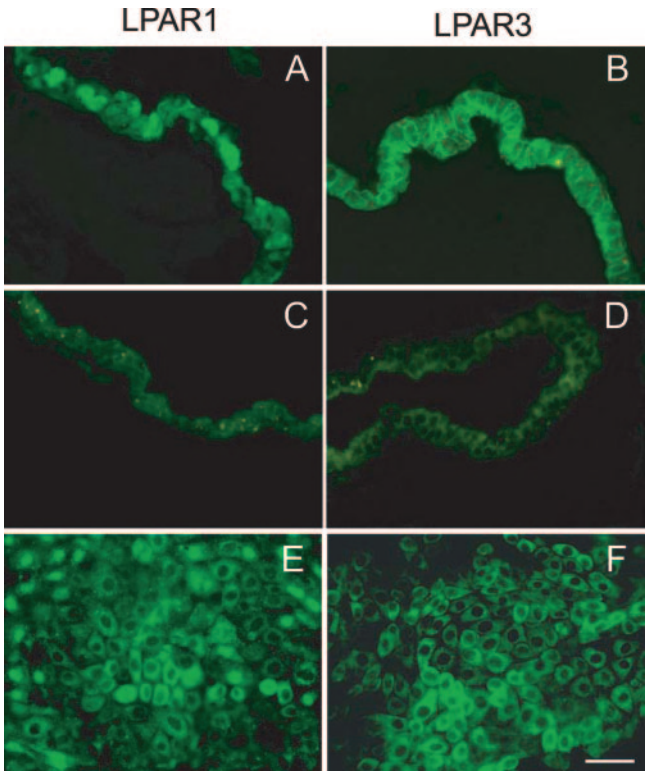

FIG. 6. Immunohistochemical localization of LPAR1 and LPAR3 in conceptuses at d 16 and in trophectoderm cells in culture. Immunofluorescent signals of LPAR1 (A) and LPAR3 (B) were detected in the trophectoderm. C and D, Controls. LPAR1 (C) and LPAR3 (D) antibodies were presaturated with the peptide antigens used to raise the polyclonal antibodies. E and F, Representative fields of preconfluent trophectoderm cells cultured on a collagen substrate with lipid-free serum. The immunofluorescent signal of LPAR1 (E) is observed in the cytoplasm of dense cells in clusters and in the nuclei of spread cells. LPAR3 (F) is localized in cytoplasm structures. *Scale bar*, 50 μm.

Activation of the ERK1/2 pathway by LPA in trophectoderm cells in culture

Because LPA has been shown to activate ERK1/2 in many cell types, we examined the ability of LPA to activate ERK1/2 in trophectoderm cells under *in vitro* conditions. LPA activated the phosphorylation of ERK1/2 in a time- and dose-dependent manner ($P = 0.022$ and $P = 0.004$, respectively; Fig. 7, A and B). Treatment with 20 μM LPA significantly stimulated a 3-fold increase in the phosphorylation of both ERK1 and ERK2 proteins. Pretreatment with VPC32183, an antagonist of LPAR1 and LPAR3 receptors, blocked the stimulatory effect of LPA on ERK1/2 phosphorylation, whereas levels of the nonphosphorylated forms of ERK1/2 were the same in control and LPA-stimulated samples (Fig. 7C). These results indicate that LPA mediates ERK1/2 activation through LPARs in trophectoderm cells.

LPA-induced proliferation in cultured ovine trophectoderm cells

LPA is the major mitogen present in serum, and it has been reported to induce cell proliferation in numerous cell systems. As shown in Fig. 8A, LPA promoted the DNA synthesis of trophec-

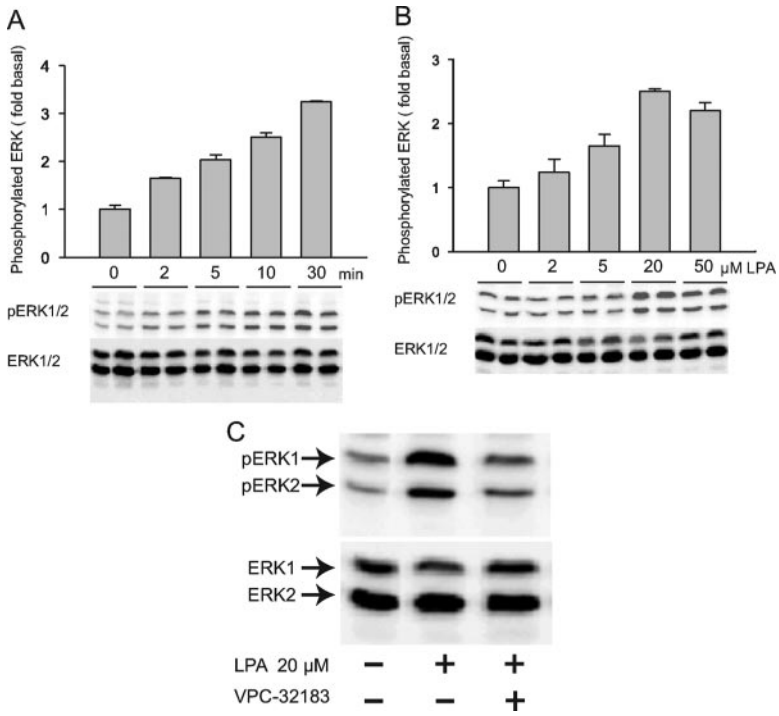

FIG. 7. Effect of LPA on the phosphorylation of ERK1/2 in trophectoderm cells in culture. Trophectoderm cells were serum starved for 24 h and then treated with LPA. A and B, Graphs show, respectively, the time effect and dose effect of LPA treatment on the phosphorylation of ERK1/2 in trophectoderm cells (two independent experiments with four cell dishes per condition were performed). Representative Western blots of phosphorylated ERK1/2 (two cell dishes per condition) are shown. LPA induced the phosphorylation of ERK1/2 in trophectoderm cells in a time- and dose-dependent manner ($P = 0.022$ and $P = 0.004$, respectively). LPA was used at 20 μM for the time-effect experiment, and the incubation period was 30 min for the dose effect experiment. C, Trophectoderm cells after starvation were pretreated or not for 30 min with 10 μM VPC32183, followed by 30 min of incubation with or without 20 μM LPA. Three independent experiments with four dishes per condition were performed. A representative Western blot using antiphospho-ERK1/2 antibodies on 15 μg of total protein extracts is shown. In all experiments, the blots were stripped and reprobed with anti-ERK1/2 antibody.

toderm cells through an increase in thymidine incorporation. The stimulation of LPA increased the proliferation of trophectoderm cells in a dose-dependent manner ($P = 0.001$). A 2-fold increase in [^{3}H]thymidine incorporation was observed after 24 h of treatment with 20–100 μM of LPA. There was thus an increase in the number of BrdU-positive cells in the presence of LPA ($P < 0.001$; Fig. 8B). The percentage of BrdU-positive cells *vs.* total nuclei stained by DAPI increased after 24 h of LPA treatment from 3.65 to 10.69%.

LPA-induced cytoskeletal changes of trophectoderm cells

LPA is known to signal through intracellular signaling pathways to affect cytoskeletal reorganization in many cell systems. The treatment of cultured ovine trophectoderm cells under serum deprivation with 20 μM LPA for 1 h led to a strong induction of stress fiber formation, promoted by β-actin polymerization (Fig. 9, A and B). Additionally, modifications to α-tubulin architecture in the cellular cytoskeleton were observed after exposure to LPA (Fig. 9, C and D).

Effect of LPA on prostaglandin synthesis by trophectoderm cells in culture

This study was performed to test the hypothesis that LPA is involved in regulating prostaglandin synthesis in ovine trophectoderm cells. Prostaglandin release was increased in a dose-dependent manner by LPA ($P = 0.0007$ and $P = 0.002$ for PGF2α and PGE2, respectively; Fig. 10A). Treatment with 20–100 μM LPA induced a 2-fold increase in the production of both PGF2α and PGE2 in the culture medium over 6 h. cPLA2α and PTGS2 are the two rate-limiting enzymes in prostaglandin synthesis, the former releasing arachidonic acid from membrane phospholipid and the latter converting the fatty acid in prostaglandin-H2 that is subsequently converted to bioactive prostaglandins. Because LPA had been found to increase prostaglandin release, we examined its effect on cPLA2α and PTGS2 gene expression (Fig. 10B). During 6 h of LPA treatment, no significant differences in cPLA2α and PTGS2 mRNA levels were observed ($P = 0.647$ and $P = 0.971$, respectively).

Discussion

For the first time, our studies investigated, the involvement of LPA pathway in early embryo development in sheep. Increased levels of LPA were detected in the ovine uterus, suggesting that the LPA pathway contributes to the intricate relationships between mother and embryo at the beginning of gestation. In humans, LPA had been identified in serum from pregnant women and its levels gradually rose until term (32). Recently the presence of different configurations of LPA has been reported in the uterus of pregnant pigs (24). In the present study, the molecular composition of LPA, which depends on the nature of the fatty acid group, has not been analyzed. However, it has never been established that the different LPA species can discriminate the diverse LPA receptors *in vivo*. In ruminants, because the two sides of the luminal epithelium are in close contact, the uterine lumen defines a virtual uterine volume. In physiological situations, the volume of fluids that accumulate in the uterine lumen is extremely low and does not exceed 1–2 ml in ewe (33). Moreover, during early pregnancy, there is a dramatic reduction in the volume of the uterine luminal fluid, which is associated with blastocyst implantation (34).

In our work, we reported that 800-1000 pmol of LPA were recovered from the uterine flush. As indicated above, if we consider that the maximal volume of uterine cavity of ewe is around 1 ml, the local concentration of LPA was, at the very least, 0.8–1 μM. These concentrations were similar to those recently reported in the porcine uterus (24) and were in the same range as the concentration we used for the *in vitro* studies. *In vitro* effect may require higher concentration of LPA that under *in vivo* conditions. LPA concentration is main-

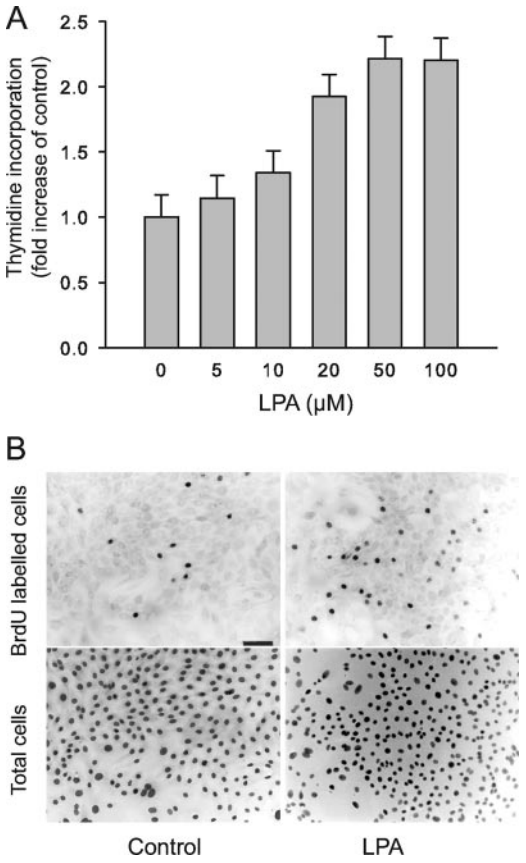

FIG. 8. Effect of LPA on the proliferation of ovine trophectoderm cells in culture. A, [^{3}H]thymidine incorporation by trophectoderm cells. Serum-starved ovine trophectoderm cells in culture were treated with different doses of LPA for 24 h and exposed for 2 additional hours to [^{3}H]thymidine (concentration 0.5 μCi/ml). Results are expressed as counts per minute/well of incorporated radiolabeled thymidine in cells treated with LPA *vs.* control cells. Graph shows the mean ± SEM of six dishes per condition. LPA increased the proliferation of trophectoderm cells in a dose-dependent manner ($P = 0.001$). B, BrdU incorporation by trophectoderm cells. Cells seeded on coverslips coated with collagen were treated for 24 h with 20 μM LPA. BrdU was added to the culture medium 1 h before the end of culture. *Black-and-white pictures* show representative fields of BrdU-labeled cells treated or not with LPA and revealed by BrdU antibody. An increase in the number of BrdU-positive cells in the presence of LPA was observed ($P < 0.001$) (see *Materials and Methods* for details).

tained by the dynamic equilibrium between production and degradation reactions. In general, under *in vitro* conditions, LPA production is lowered due to the lower availability of substrate (lysophosphatidylcholine), but the degradation reactions are still fully operational. This makes the concentration of exogenously added LPA less stable along time. Thus, *in vitro* experiments require higher LPA concentration to minimize the impact of its rapid degradation.

LPA can be produced under various conditions in both cells and biological fluids. At least two pathways of LPA synthesis have been proposed, in which enzymes from the phospholipase family participate. One is the sequential action of phospholipase-D and phospholipase-A1 or -A2. Another route involves phospholipase-A1 or -A2 followed by autotaxin (35). The disruption of the autotaxin-encoding gene has identified this enzyme as that responsible for the extracellular production of LPA (36, 37). During our experiments, autotaxin was found to be expressed by the uterus and conceptus. Autotaxin levels were 4- to 5-fold higher in the uterus than the trophectoderm. The apical localization of autotaxin in uterine cells of glands and luminal epithelium indicates that the lysophospholipase-D activity of autotaxin is orientated toward the uterine lumen. Taken together, these findings suggest that the extracellular production of LPA detected in the ovine uterus may be due to lysophospholipase-D activity on the maternal side. However, the elevating expression of autotaxin in conceptuses, which paralleled the increasing level of LPA within the uterus, indicates that the trophectoderm may also contribute to the production of LPA during pregnancy.

In humans, autotaxin has been found to be highly expressed in the placenta (8), and the elevated levels of serum LPA found during pregnancy were reported to arise from both the placenta and the fetus (32). During embryonic development in mice, the analysis of autotaxin mRNA expression identified the yolk sac and embryo as sources of autotaxin, which was consequently found in amniotic fluids. In the ovine conceptus, trophectoderm cells were identified as a source of the autotaxin because we detected it in both the mRNA and protein of the enzyme in these cells. Autotaxin-deficient mice were shown to be lethal, with profound vascular defects in the yolk sac and embryo (36, 37). In sheep, vasculogenesis occurs first in the yolk sac by d 15–17 and then extends to the embryo and allantoic membranes. Our data indicating an increased expression of autotaxin at the time of yolk sac formation suggest that autotaxin could also be involved in vascular development during pregnancy in sheep.

The potential role of LPA would depend on both its local concentration and the distribution of its receptors. LPARs are widely and differentially expressed in embryonic and adult tissues (11). In the present study, we have described the gene expression profile of three LPARs in the ovine trophectoderm during the perimplantation period. Two of them (LPAR1 and LPAR3) exhibited a strictly regulated pattern of expression. We observed high and narrow peaks for transcripts levels at d 14 of embryonic development, the increase in protein levels being delayed by 1 or 2 d. A similar time interval between peak expression of the protein and the transcript had previously been reported for the major product secreted by the trophectoderm of the sheep embryo, *i.e.* interferon-τ. Embryonic interferon mRNA has been found to be most abundant at d 14, whereas the interferon protein reaches its highest levels on d 16–18 when the RNA is almost undetectable (38, 39). Our data suggest that in the ovine conceptus, the function of LPA is largely controlled at the level of LPA receptor expression. Because LPAR1 and LPAR3 expressions were found to be regulated during early pregnancy, one possibility is that these receptors are under steroid hormone control in the same way as uterine LPAR3 in mice (40) and pigs (24). Furthermore, because embryo implantation is regarded as a proinflammatory situation and occurs in a cytokine-rich environment (41, 42), cytokines may also be involved in the induction of LPARs. In human synoviocytes, LPAR3 receptors have been shown to be up-regulated by the inflammatory cytokine TNF-α (43). LPA has been reported as being both an extracellular mediator and intracellular messenger because distinct sources of LPA exist in the extracellular environment and cellular

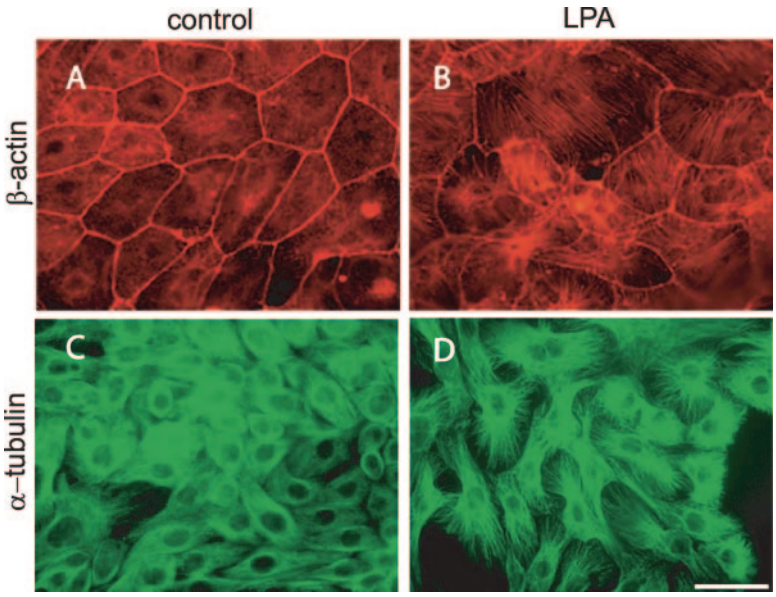

FIG. 9. Effect of LPA on cultured ovine trophectoderm cell morphology. Cultures of ovine trophectoderm cells maintained under serum deprivation were treated with 20 μM LPA for 1 h and stained for β-actin (B) or α-tubulin (D). LPA induced formation of stress fiber promoted by β-actin polymerization (B) and modifications to α-tubulin architecture (D). A and C, Organization of the β-actin (A) and α-tubulin (C) networks in control cells not exposed to LPA. Representative fields of trophectoderm cells from two independent experiments are shown. *Scale bar*, 50 μm.

cytosol (44, 45). Moreover, the detection of LPA receptors on the cell surface and in intracellular compartments suggests a dual action of the lipid mediator (46, 47). Our experiments revealed perinuclear/nuclear and membrane localizations of LPAR1 in ovine conceptuses and trophectoderm cells cultivated *in vitro*, whereas LPAR3 was found only in the cell membrane in both systems, which is in agreement with previously published reports (46, 47). The nuclear localization of LPAR1 has been reported to be related to cell density (47) or to result from translocation from the cell membrane to the nucleus in response to LPA (48). The nuclear localization of LPAR1suggests that it may be involved in regulating intranuclear protein phosphorylation and signaling.

Our results revealed that LPA stimulated the phosphorylation of ERK1/2 in ovine trophectoderm cells under *in vitro* conditions, and a specific antagonist of LPAR1 and LPAR3 receptors (VPC32183) blocked this effect. These observations provide direct evidence that LPARs operate and are functionally coupled to signal transduction mechanisms in the trophectoderm cell. The activation of ERK1/2 has been already reported in numerous cell types [fibroblasts (49, 50), neuroblastoma cells (51), leiomyoma cells (28)] and is commonly related to the proliferative effect of LPA. During the periimplantation period, the sheep blastocyst undergoes rapid trophectoderm development from d 12 to 16, resulting in a filamentous conceptus (52). The size of the conceptus increases more than 1000-fold during this elongation period that requires the intense proliferation of trophectoderm cells. Our results that demonstrated a proliferative effect of LPA on trophectoderm cells support the hypothesis that the lysophospholipid could be involved in this elongation phase. In ovine conceptuses, we observed a time correlation between the phosphorylation of ERK1/2 and the up-regulation of LPA membrane receptors (data not shown). However, it is not certain that, *in vivo*, LPA is solely responsible for the phosphorylation state of MAPKs observed because the conceptus develops in a uterine environment that is rich in many factors that can induce ERK1/2 phosphorylation. ERK1/2 MAPKs have been found to be widely expressed throughout early-stage embryo development and have been suggested as participating in trophectoderm development in both mice (53) and humans (54). In addition to its role in the proliferation of trophectoderm cells during the elongation phase, LPA could also be involved in mediating the cellular differentiation required for ovine embryo implantation. In mice, LPA accelerates the rate of trophectoderm outgrowth (55, 56), and it induces an accumulation of heparin binding epidermal growth factor on the embryo surface (55), which has been reported to be involved in embryo implantation in several species (57–59).

In contrast to primates and rodents with invasive implantation, sheep has superficial implantation in which a prolonged preattachment period (~15 d) is followed by incremental apposition and attachment (21). Initiation of implantation involves adhesion of trophectoderm cells to the epithelial lining of the endometrium (21, 22). In mice, the trophectoderm adhesion is distinguished by dramatic changes in cytoarchitecture and cell behavior including actin stress fiber formation (60). However the mechanisms regulating the adhesive properties of trophectoderm during initiation of implantation are still incompletely understood. Many literature reports demonstrated a role of LPA in cytoskeletal rearrangement of numerous cell systems (61, 62). We report here on ovine trophectoderm cells under *in vitro* conditions that LPA stimulates changes in the organization of actin and tubulin architecture. These results give new insight into the role of bioactive lipid mediators in the implantation process and suggest that LPA may be involved in the mechanisms regulating morphological changes during conceptus adhesion to the uterus in ruminants.

Our studies revealed that LPA induced a 2-fold increase in PGF2α and PGE2 release from ovine trophectoderm cells in culture. However, with an incubation period of the same duration, no increase in the gene expression of cPLA2α and PTGS2 was observed. Using a shorter incubation period, the LPA-mediated increase in prostaglandin synthesis was already detected (data not shown). These results exclude the hypothesis that short-term effect of LPA on prostaglandin release is due to changes in mRNA of the two enzymes. Numerous reports have proposed that the phosphorylation of cPLA2α by ERK1/2 is a critical step in the sequence of events leading to the mobilization of arachidonic acid (63, 64). In trophectoderm cells, the LPA-mediated phosphorylation of ERK1/2 may cause a rapid activation of cPLA2α that results in a burst of prostaglandin synthesis independently of any modifications to gene expression. LPA has previously been shown to increase PGE2 synthesis in human monocytic cells (65) and mesangial cells (66) and up-regulate PTGS2 expression in other cell types such as human ovarian

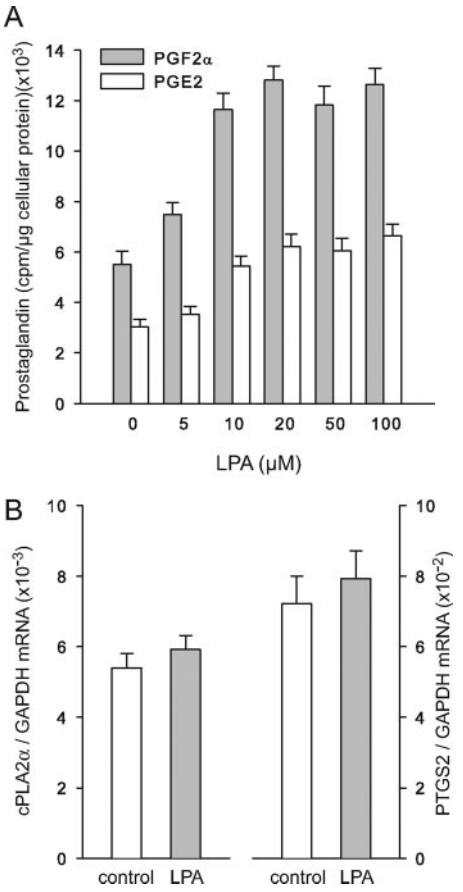

FIG. 10. Effect of LPA on prostaglandin production by trophectoderm cells in culture and on cPLA2α and PTGS2 expression A, Trophectoderm cells were treated for 6 h with different doses of LPA in the presence of radiolabeled arachidonic acid. The culture medium was collected and extracted, and cyclooxygenate derivatives were analyzed by HPLC. Histogram represents PGF2α and PGE2 production per counts per minute per microgram of cellular protein in trophectoderm cells (n = 4). LPA induced an increase in the production of PGF2α and PGE2 in the culture medium over 6 h ($P = 0.0007$ and $P = 0.002$, respectively). B, Trophectoderm cells were treated for 6 h with or without 20 μM LPA. The graph presents real-time quantitative RT-PCR measurements of cPLA2α and PTGS2 gene expression from four independent experiments performed in triplicate. Each transcript level was normalized to GAPDH. No significant differences in cPLA2α and PTGS2 mRNA levels were observed ($P = 0.647$ and $P = 0.971$, respectively) after LPA treatment.

cancer cells (67) and rat mesangial cells (68). If emerging evidence suggests that LPA is a regulator of prostaglandin synthesis and PTGS2 expression, other ways mechanisms have also been put forward. LPA has been shown to regulate PTGS2 expression via the transactivation of epidermal growth factor (69) and the enhancement of mRNA stability (70). In mice, the targeted deletion of LPAR3 resulted in implantation defects accompanied by a reduction in PTGS2 expression and levels of PGE2 and PGI2 (6). Moreover, the improvement in implantation achieved by the exogenous delivery of prostaglandins in LPAR3-deficient mice have rendered the LPA-induced PTGS2 expression of prime importance for embryo implantation. In sheep, it is unlikely that the same pathway will prove to be relevant. In the ovine conceptus, PTGS2 reaches its highest levels on d 15 of embryonic development (26), whereas we found maximum levels of LPAR1 and LPAR3 proteins 2 d later at d 17. These findings thus lead us to suppose that LPA-mediated signaling does not induce PTGS2 expression in the ovine conceptus. The LPA-induced release of prostaglandin is probably due to a stimulation of arachidonic acid mobilization. Taken together, the combination of a strong expression of both the PTGS2 enzyme and LPARs may lead to a synergetic effect that results in a massive synthesis of prostaglandins in the presence of increasing amounts of LPA in the uterine lumen.

Overall, our results designate a new biological function for LPA in embryonic development and a key role in the regulation of prostaglandin levels during the implantation process. Our studies establish, in a mammalian species other than the mouse, the importance of lipid signaling in implantation. It is still necessary to clarify how prostaglandins of embryonic origin control embryo-uterus interactions during implantation in sheep. In ruminant, prostaglandins are known to play a pivotal role in luteolysis maintenance, maternal, and recognition of pregnancy. The uterine source of prostaglandins has been extensively studied, but little is known about prostaglandins originated from embryo and conceptus. In ruminant, the prostaglandin production has been reported from cumulus-oocyte complex stage (71, 72), early blastocyst (73), through to elongated conceptus (25, 74, 75). PGE2 has been shown to increase the hatching rate of ovine blastocysts (73), whereas PGF2α has been reported to be detrimental to the development of the early bovine blastocyst (76). However, the function of prostaglandins during the elongation of the ruminant trophectoderm are not understood. PGE2 had been reported to regulate proliferation and migration of human trophoblast (77, 78).

Of the two main defects observed in LPAR3-deficient mice, delayed implantation and embryo crowding, the exogenous delivery of prostaglandins rescued normal implantation but not the defect of embryo spacing. Despite significant differences between implantation in the mouse and ruminant, prostaglandins may mediate similar mechanisms. In sheep, intrauterine migration of embryos into the uterine horn contralateral to the ovary was observed only when two or more ovulations occurred in one ovary (79). However, in this species, a role of LPA in the mechanisms of embryo spacing and migration is unlikely because migration was completed by d 15 (80) and occurred before LPA signaling takes place.

Acknowledgments

The authors thank the staff of Unité commune d'expérimentation animale farms and the slaughterhouse for their help with the ewes, and Guy Germain for his critical reading of the manuscript.

Address all correspondence and requests for reprints to: Gilles Charpigny, Institut National de la Recherche Agronomique, Unité Mixte de Recherche 1198 Biologie du Développement et Reproduction, F-78350 Jouy en Josas, France. E-mail: gilles.charpigny@jouy.inra.fr.

E.L. was supported by a fellowship from Regulation and Variability of Animal Genome Expression, a Marie Curie Early Stage Research Training action under the European Community Sixth Framework Program (FP6).

Disclosure Statement: The authors have nothing to disclose.

References

1. **van Meeteren LA, Moolenaar WH** 2007 Regulation and biological activities of the autotaxin-LPA axis. Prog Lipid Res 46:145–160
2. **Budnik LT, Mukhopadhyay AK** 2002 Lysophosphatidic acid-induced nuclear localization of protein kinase CΔ in bovine theca cells stimulated with luteinizing hormone. Biol Reprod 67:935–944
3. **Hinokio K, Yamano S, Nakagawa K, Iraharaa M, Kamada M, Tokumura A, Aono T** 2002 Lysophosphatidic acid stimulates nuclear and cytoplasmic maturation of golden hamster immature oocytes *in vitro* via cumulus cells. Life Sci 70:759–767
4. **Kunikata K, Yamano S, Tokumura A, Aono T** 1999 Effect of lysophosphatidic acid on the ovum transport in mouse oviducts. Life Sci 65:833–840
5. **Kobayashi T, Yamano S, Murayama S, Ishikawa H, Tokumura A, Aono T** 1994 Effect of lysophosphatidic acid on the preimplantation development of mouse embryos. FEBS Lett 351:38–40
6. **Ye X, Hama K, Contos JJ, Anliker B, Inoue A, Skinner MK, Suzuki H, Amano T, Kennedy G, Arai H, Aoki J, Chun J** 2005 LPA3-mediated lysophosphatidic acid signalling in embryo implantation and spacing. Nature 435:104–108
7. **Tokumura A, Majima E, Kariya Y, Tominaga K, Kogure K, Yasuda K, Fukuzawa K** 2002 Identification of human plasma lysophospholipase D, a lysophosphatidic acid-producing enzyme, as autotaxin, a multifunctional phosphodiesterase. J Biol Chem 277:39436–39442
8. **Lee HY, Murata J, Clair T, Polymeropoulos MH, Torres R, Manrow RE, Liotta LA, Stracke ML** 1996 Cloning, chromosomal localization, and tissue expression of autotaxin from human teratocarcinoma cells. Biochem Biophys Res Commun 218:714–719
9. **Pradere JP, Tarnus E, Gres S, Valet P, Saulnier-Blache JS** 2007 Secretion and lysophospholipase D activity of autotaxin by adipocytes are controlled by N-glycosylation and signal peptidase. Biochim Biophys Acta 1771:93–102
10. **Tokumura A** 2002 Physiological and pathophysiological roles of lysophosphatidic acids produced by secretory lysophospholipase D in body fluids. Biochim Biophys Acta 1582:18–25
11. **Meyer zu Heringdorf D, Jakobs KH** 2007 Lysophospholipid receptors: signalling, pharmacology and regulation by lysophospholipid metabolism. Biochim Biophys Acta 1768:923–940
12. **Noguchi K, Ishii S, Shimizu T** 2003 Identification of p2y9/GPR23 as a novel G protein-coupled receptor for lysophosphatidic acid, structurally distant from the Edg family. J Biol Chem 278:25600–25606
13. **Lee CW, Rivera R, Gardell S, Dubin AE, Chun J** 2006 GPR92 as a new G12/13- and Gq-coupled lysophosphatidic acid receptor that increases cAMP, LPA5. J Biol Chem 281:23589–23597
14. **van Corven EJ, Groenink A, Jalink K, Eichholtz T, Moolenaar WH** 1989 Lysophosphatidate-induced cell proliferation: identification and dissection of signaling pathways mediated by G proteins. Cell 59:45–54
15. **Anliker B, Chun J** 2004 Cell surface receptors in lysophospholipid signaling. Semin Cell Dev Biol 15:457–465
16. **Yang AH, Ishii I, Chun J** 2002 *In vivo* roles of lysophospholipid receptors revealed by gene targeting studies in mice. Biochim Biophys Acta 1582: 197–203
17. **Contos JJ, Fukushima N, Weiner JA, Kaushal D, Chun J** 2000 Requirement for the lpA1 lysophosphatidic acid receptor gene in normal suckling behavior. Proc Natl Acad Sci USA 97:13384–13389
18. **Contos JJ, Ishii I, Fukushima N, Kingsbury MA, Ye X, Kawamura S, Brown JH, Chun J** 2002 Characterization of lpa(2) (Edg4) and lpa(1)/lpa(2) (Edg2/Edg4) lysophosphatidic acid receptor knockout mice: signaling deficits without obvious phenotypic abnormality attributable to lpa(2). Mol Cell Biol 22: 6921–6929
19. **Song H, Lim H, Paria BC, Matsumoto H, Swift LL, Morrow J, Bonventre JV, Dey SK** 2002 Cytosolic phospholipase A2α is crucial [correction of A2α deficiency is crucial] for 'on-time' embryo implantation that directs subsequent development. Development 129:2879–2889
20. **Lim H, Paria BC, Das SK, Dinchuk JE, Langenbach R, Trzaskos JM, Dey SK** 1997 Multiple female reproductive failures in cyclooxygenase 2-deficient mice. Cell 91:197–208
21. **Spencer TE, Johnson GA, Bazer FW, Burghardt RC** 2004 Implantation mechanisms: insights from the sheep. Reproduction 128:657–668
22. **Guillomot M, Flechon JE, Wintenberger-Torres S** 1981 Conceptus attachment in the ewe: an ultrastructural study. Placenta 2:169–182
23. **Kaminska K, Wasielak M, Bogacka I, Blitek M, Bogacki M** 2008 Quantitative expression of lysophosphatidic acid receptor 3 gene in porcine endometrium during the periimplantation period and estrous cycle. Prostaglandins Other Lipid Mediat 85:26–32
24. **Seo H, Kim M, Choi Y, Lee CK, Ka H** 2008 Analysis of lysophosphatidic acid receptor and lysophosphatidic acid-induced endometrial PTGS2 expression in the porcine uterus. Endocrinology 149:6166–6175
25. **Charpigny G, Reinaud P, Tamby JP, Creminon C, Guillomot M** 1997 Cyclooxygenase-2 unlike cyclooxygenase-1 is highly expressed in ovine embryos during the implantation period. Biol Reprod 57:1032–1040
26. **Charpigny G, Reinaud P, Tamby JP, Creminon C, Martal J, Maclouf J, Guillomot M** 1997 Expression of cyclooxygenase-1 and -2 in ovine endometrium during the estrous cycle and early pregnancy. Endocrinology 138:2163–2171
27. **Saulnier-Blache JS, Girard A, Simon MF, Lafontan M, Valet P** 2000 A simple and highly sensitive radioenzymatic assay for lysophosphatidic acid quantification. J Lipid Res 41:1947–1951
28. **Billon-Denis E, Tanfin Z, Robin P** 2008 Role of lysophosphatidic acid in the regulation of uterine leiomyoma cell proliferation by phospholipase D and autotaxin. J Lipid Res 49:295–307
29. **Chomczynski P, Sacchi N** 1987 Single-step method of RNA isolation by acid guanidinium thiocyanate-phenol-chloroform extraction. Anal Biochem 162: 156–159
30. **Cammas L, Reinaud P, Bordas N, Dubois O, Germain G, Charpigny G** 2006 Developmental regulation of prostacyclin synthase and prostacyclin receptors in the ovine uterus and conceptus during the peri-implantation period. Reproduction 131:917–927
31. **Charpigny G, Reinaud P, Creminon C, Tamby JP** 1999 Correlation of increased concentration of ovine endometrial cyclooxygenase 2 with the increase in PGE2 and PGD2 in the late luteal phase. J Reprod Fertil 117:315–324
32. **Tokumura A, Kanaya Y, Miyake M, Yamano S, Irahara M, Fukuzawa K** 2002 Increased production of bioactive lysophosphatidic acid by serum lysophospholipase D in human pregnancy. Biol Reprod 67:1386–1392
33. **Menezo Y** 1981 Sécrétions utérines associées à la phase périovulatoire et à la vie libre des blastocystes. In: Boury-Heyler C, Mauléon P, Rochet Y, eds. Utérus et fécondité. Paris: Masson; 3–16
34. **Enders A, Schlafke S** 1967 A morphological analysis of the early implantation stages in the rat. Am J Anat 120:185–226
35. **Aoki J** 2004 Mechanisms of lysophosphatidic acid production. Semin Cell Dev Biol 15:477–489
36. **van Meeteren LA, Ruurs P, Stortelers C, Bouwman P, van Rooijen MA, Pradere JP, Pettit TR, Wakelam MJ, Saulnier-Blache JS, Mummery CL, Moolenaar WH, Jonkers J** 2006 Autotaxin, a secreted lysophospholipase D, is essential for blood vessel formation during development. Mol Cell Biol 26:5015–5022
37. **Tanaka M, Okudaira S, Kishi Y, Ohkawa R, Iseki S, Ota M, Noji S, Yatomi Y, Aoki J, Arai H** 2006 Autotaxin stabilizes blood vessels and is required for embryonic vasculature by producing lysophosphatidic acid. J Biol Chem 281: 25822–25830
38. **Hansen TR, Imakawa K, Polites HG, Marotti KR, Anthony RV, Roberts RM** 1988 Interferon RNA of embryonic origin is expressed transiently during early pregnancy in the ewe. J Biol Chem 263:12801–12804
39. **Kazemi M, Malathy PV, Keisler DH, Roberts RM** 1988 Ovine trophoblast protein-1 and bovine trophoblast protein-1 are present as specific components of uterine flushings of pregnant ewes and cows. Biol Reprod 39:457–463
40. **Hama K, Aoki J, Bandoh K, Inoue A, Endo T, Amano T, Suzuki H, Arai H** 2006 Lysophosphatidic receptor, LPA3, is positively and negatively regulated by progesterone and estrogen in the mouse uterus. Life Sci 79:1736–1740
41. **Ingman WV, Jones RL** 2008 Cytokine knockouts in reproduction: the use of gene ablation to dissect roles of cytokines in reproductive biology. Hum Reprod Update 14:179–192
42. **Chaouat G, Dubanchet S, Ledee N** 2007 Cytokines: important for implantation? J Assist Reprod Genet 24:491–505
43. **Zhao C, Fernandes MJ, Prestwich GD, Turgeon M, Di Battista J, Clair T, Poubelle PE, Bourgoin SG** 2008 Regulation of lysophosphatidic acid receptor expression and function in human synoviocytes: implications for rheumatoid arthritis? Mol Pharmacol 73:587–600
44. **Tokumura A** 2004 Metabolic pathways and physiological and pathological significances of lysolipid phosphate mediators. J Cell Biochem 92:869–881
45. **Xu YJ, Rathi SS, Chapman DC, Arneja AS, Dhalla NS** 2003 Mechanisms of lysophosphatidic acid-induced DNA synthesis in vascular smooth muscle cells. J Cardiovasc Pharmacol 41:381–387
46. **Gobeil Jr F, Bernier SG, Vazquez-Tello A, Brault S, Beauchamp MH, Quiniou C, Marrache AM, Checchin D, Sennlaub F, Hou X, Nader M, Bkaily G, Ribeiro-da-Silva A, Goetzl EJ, Chemtob S** 2003 Modulation of pro-inflammatory gene expression by nuclear lysophosphatidic acid receptor type-1. J Biol Chem 278:38875–38883
47. **Waters CM, Saatian B, Moughal NA, Zhao Y, Tigyi G, Natarajan V, Pyne S, Pyne NJ** 2006 Integrin signalling regulates the nuclear localization and func-

tion of the lysophosphatidic acid receptor-1 (LPA1) in mammalian cells. Biochem J 398:55–62
48. **Moughal NA, Waters C, Sambi B, Pyne S, Pyne NJ** 2004 Nerve growth factor signaling involves interaction between the Trk A receptor and lysophosphatidate receptor 1 systems: nuclear translocation of the lysophosphatidate receptor 1 and Trk A receptors in pheochromocytoma 12 cells. Cell Signal 16:127–136
49. **Kumagai N, Morii N, Fujisawa K, Yoshimasa T, Nakao K, Narumiya S** 1993 Lysophosphatidic acid induces tyrosine phosphorylation and activation of MAP-kinase and focal adhesion kinase in cultured Swiss 3T3 cells. FEBS Lett 329:273–276
50. **Hordijk PL, Verlaan I, van Corven EJ, Moolenaar WH** 1994 Protein tyrosine phosphorylation induced by lysophosphatidic acid in rat-1 fibroblasts. Evidence that phosphorylation of MAP kinase is mediated by the Gi-p21ras pathway. J Biol Chem 269:645–651
51. **Ishii I, Contos JJ, Fukushima N, Chun J** 2000 Functional comparisons of the lysophosphatidic acid receptors, LP(A1)/VZG-1/EDG-2, LP(A2)/EDG-4, and LP(A3)/EDG-7 in neuronal cell lines using a retrovirus expression system. Mol Pharmacol 58:895–902
52. **Blomberg L, Hashizume K, Viebahn C** 2008 Blastocyst elongation, trophoblastic differentiation, and embryonic pattern formation. Reproduction 135: 181–195
53. **Saba-El-Leil MK, Vella FD, Vernay B, Voisin L, Chen L, Labrecque N, Ang SL, Meloche S** 2003 An essential function of the mitogen-activated protein kinase Erk2 in mouse trophoblast development. EMBO Rep 4:964–968
54. **Daoud G, Amyot M, Rassart E, Masse A, Simoneau L, Lafond J** 2005 ERK1/2 and p38 regulate trophoblasts differentiation in human term placenta. J Physiol 566:409–423
55. **Liu Z, Armant DR** 2004 Lysophosphatidic acid regulates murine blastocyst development by transactivation of receptors for heparin-binding EGF-like growth factor. Exp Cell Res 296:317–326
56. **Shiokawa S, Sakai K, Akimoto Y, Suzuki N, Hanashi H, Nagamatsu S, Iwashita M, Nakamura Y, Hirano H, Yoshimura Y** 2000 Function of the small guanosine triphosphate-binding protein RhoA in the process of implantation. J Clin Endocrinol Metab 85:4742–4749
57. **Tamada H, Higashiyama C, Takano H, Kawate N, Inaba T, Sawada T** 1999 The effects of heparin-binding epidermal growth factor-like growth factor on preimplantation-embryo development and implantation in the rat. Life Sci 64:1967–1973
58. **Klonisch T, Wolf P, Hombach-Klonisch S, Vogt S, Kuechenhoff A, Tetens F, Fischer B** 2001 Epidermal growth factor-like ligands and erbB genes in the peri-implantation rabbit uterus and blastocyst. Biol Reprod 64:1835–1844
59. **Wang X, Wang H, Matsumoto H, Roy SK, Das SK, Paria BC** 2002 Dual source and target of heparin-binding EGF-like growth factor during the onset of implantation in the hamster. Development 129:4125–4134
60. **Parast MM, Aeder S, Sutherland AE** 2001 Trophoblast giant-cell differentiation involves changes in cytoskeleton and cell motility. Dev Biol 230:43–60
61. **Sah VP, Seasholtz TM, Sagi SA, Brown JH** 2000 The role of Rho in G protein-coupled receptor signal transduction. Annu Rev Pharmacol Toxicol 40:459–489
62. **Moolenaar WH** 2000 Development of our current understanding of bioactive lysophospholipids. Ann NY Acad Sci 905:1–10
63. **An S, Bleu T, Hallmark OG, Goetzl EJ** 1998 Characterization of a novel subtype of human G protein-coupled receptor for lysophosphatidic acid. J Biol Chem 273:7906–7910
64. **Kramer RM, Sharp JD** 1997 Structure, function and regulation of Ca2+-sensitive cytosolic phospholipase A2 (cPLA2). FEBS Lett 410:49–53
65. **D'Aquilio F, Procaccini M, Izzi V, Chiurchiu V, Giambra V, Carotenuto F, Di Nardo P, Baldini PM** 2007 Activatory properties of lysophosphatidic acid on human THP-1 cells. Inflammation 30:167–177
66. **Inoue CN, Forster HG, Epstein M** 1995 Effects of lysophosphatidic acid, a novel lipid mediator, on cytosolic Ca2+ and contractility in cultured rat mesangial cells. Circ Res 77:888–896
67. **Symowicz J, Adley BP, Woo MM, Auersperg N, Hudson LG, Stack MS** 2005 Cyclooxygenase-2 functions as a downstream mediator of lysophosphatidic acid to promote aggressive behavior in ovarian carcinoma cells. Cancer Res 65:2234–2242
68. **Reiser CO, Lanz T, Hofmann F, Hofer G, Rupprecht HD, Goppelt-Struebe M** 1998 Lysophosphatidic acid-mediated signal-transduction pathways involved in the induction of the early-response genes prostaglandin G/H synthase-2 and Egr-1: a critical role for the mitogen-activated protein kinase p38 and for Rho proteins. Biochem J 330(Pt 3):1107–1114
69. **He D, Natarajan V, Stern R, Gorshkova IA, Solway J, Spannhake EW, Zhao Y** 2008 Lysophosphatidic acid-induced transactivation of epidermal growth factor receptor regulates cyclo-oxygenase-2 expression and prostaglandin E(2) release via C/EBPβ in human bronchial epithelial cells. Biochem J 412:153–162
70. **Oyesanya RA, Lee ZP, Wu J, Chen J, Song Y, Mukherjee A, Dent P, Kordula T, Zhou H, Fang X** 2008 Transcriptional and post-transcriptional mechanisms for lysophosphatidic acid-induced cyclooxygenase-2 expression in ovarian cancer cells. FASEB J 22:2639–2651
71. **Gurevich M, Harel-Markowitz E, Marcus S, Shore LS, Shemesh M** 1993 Prostaglandin production by the oocyte cumulus complex around the time of fertilization and the effect of prostaglandin E on the development of the early bovine embryo. Reprod Fertil Dev 5:281–283
72. **Nuttinck F, Reinaud P, Tricoire H, Vigneron C, Peynot N, Mialot JP, Mermillod P, Charpigny G** 2002 Cyclooxygenase-2 is expressed by cumulus cells during oocyte maturation in cattle. Mol Reprod Dev 61:93–101
73. **Sayre BL, Lewis GS** 1993 Arachidonic acid metabolism during early development of ovine embryos: a possible relationship to shedding of the zona pellucida. Prostaglandins 45:557–569
74. **Lewis GS, Thatcher WW, Bazer FW, Curl JS** 1982 Metabolism of arachidonic acid *in vitro* by bovine blastocysts and endometrium. Biol Reprod 27:431–439
75. **Hwang DH, Pool SH, Rorie RW, Boudreau M, Godke RA** 1988 Transitional changes in arachidonic acid metabolism by bovine embryos at different developmental stages. Prostaglandins 35:387–402
76. **Scenna FN, Edwards JL, Rohrbach NR, Hockett ME, Saxton AM, Schrick FN** 2004 Detrimental effects of prostaglandin F2α on preimplantation bovine embryos. Prostaglandins Other Lipid Mediat 73:215–226
77. **Nicola C, Chirpac A, Lala PK, Chakraborty C** 2008 Roles of Rho guanosine 5′-triphosphatase A, Rho kinases, and extracellular signal regulated kinase (1/2) in prostaglandin E2-mediated migration of first-trimester human extravillous trophoblast. Endocrinology 149:1243–1251
78. **Biondi C, Ferretti ME, Pavan B, Lunghi L, Gravina B, Nicoloso MS, Vesce F, Baldassarre G** 2006 Prostaglandin E2 inhibits proliferation and migration of HTR-8/SVneo cells, a human trophoblast-derived cell line. Placenta 27: 592–601
79. **Casida LE, Woody CO, Pope AL** 1966 Inequality in function of the right and left ovaries and uterine horns of the ewe. J Anim Sci 25:1169–1171
80. **Nephew KP, McClure KE, Pope WF** 1989 Embryonic migration relative to maternal recognition of pregnancy in sheep. J Anim Sci 67:999–1005